J MATER SCI **41** (2006) 2673–2677

Transmission electron microscopy study on the superstructure and the precipitation of γ'-Fe_4N in initially homogeneous ε-iron nitride powders

Z. Q. LIU*
High Voltage Electron Microscopy Station, National Institute for Materials Science, Sakura 3-13, Tsukuba 305-0003, Japan
E-mail: zhiquanliu@yahoo.com, liu.zhiquan@nims.go.jp

A. LEINEWEBER
Max Planck Institute for Metals Research, Heisenbergstraβe 3, 70569, Stuttgart, Germany

K. MITSUISHI, K. FURUYA
High Voltage Electron Microscopy Station, National Institute for Materials Science, Sakura 3-13, Tsukuba 305-0003, Japan

Published online: 17 April 2006

Annealed and quenched ε-$Fe_{2-3}N$ powders with an initially homogeneous composition of $Fe_3N_{1.0}$ were studied by transmission electron microscopy (TEM). TEM specimens were successfully prepared from the powder using a sandwiching technique. The superstructure in ε-powders was identified as ε'-Fe_3N type (space group $P6_322$), and no other type of superstructure was observed. γ'-Fe_4N nitride precipitated from ε powders as individual grains during the annealing process, which is different from the typical fine lamellar structure observed in bulk iron-nitride samples. The observed orientation relationships between γ' and ε grains are also different from that reported in the lamellar structure of bulk iron-nitride samples. This suggests that in the powder investigated by us there is no one specific orientation of the precipitated γ' grains with respect to the parent ε grains.

1. Introduction

Due to their benefit in the surface modification of iron and steel and their potential as magnetic recording materials, iron nitrides have been investigated extensively in the past several decades. The microstructure of the surface layer of the nitride bulk sample varies with different nitriding methods and procedures. In the general case with sufficient nitrogen, the nitride layer of iron and steel contains an outermost compound layer and an inner diffusion layer [1, 2]. The nitride compound layer is composed of ε-$Fe_{2-3}N$ (with a hexagonal structure) and γ'-Fe_4N (with a cubic structure), while in the diffusion layer γ'-Fe_4N and α''-$Fe_{16}N_2$ (with a tetragonal structure) precipitate from α-Fe substrate [3, 4]. In the Fe-N phase diagram the ε-$Fe_{2-3}N$ nitride has a wide homogeneity range from 18 to 33 at% nitrogen [5, 6]. The variation of nitrogen occupancy in the octahedral interstices of the iron sublattice, can result in different superstructures in ε-$Fe_{2-3}N$ according to X-ray diffraction [6–8]. This has also been studied by electron microscopy on the surface iron-nitride layers grown on iron [9–12]. However, due to the existence of a nitrogen gradient from the surface to the interior, which is induced by the inwards diffusion process of nitrogen into the solid, it is hard to determine the nitrogen concentration of the local area of the layer chosen for investigation of the superstructure. On the other hand, homogeneous ε-$Fe_{2-3}N$ powders can be prepared by nitriding of iron powders. Their compositions can be easily determined, which is very useful for the investigation of the interdependence between the nitrogen-superstructure and composition, as

*Author to whom all correspondence should be addressed.
0022-2461
DOI: 10.1007/s10853-006-7869-9

studied on such samples by neutron diffraction [13, 14]. Moreover, it has been reported that precipitation of γ'-Fe_4N inside ε-$Fe_{2-3}N$ grains in bulk samples results in a lamellar morphology of grains [4, 15]. However, the details of this process in homogeneous powder samples are not yet clear. In the present paper, transmission electron microscopy (TEM) was used to study the superstructure and the precipitation of γ'-Fe_4N in ε-powders with an initially homogeneous composition of $Fe_3N_{1.0}$.

2. Experimental

The iron nitride powders used in the present studies were prepared as described previously from iron powder (particle size 1–5 μm, Alfa, 99.9%) and $NH_3/H_2/N_2$ mixtures [14, 16]. The composition of as-prepared ε-powders is $Fe_3N_{1.0}$, as determined by chemical analysis. Annealing of this powder was carried out in evacuated quartz tubes at 657 K for up to 4 days, followed by quenching to room temperature. This leads—as evidenced by X-ray powder diffraction and as expected from the phase diagram [5]—to the formation of γ'-Fe_4N and the enrichment of nitrogen in the ε-phase giving a final composition of about $Fe_3N_{1.1}$ [17].

TEM specimens of the powders were prepared by a cross-sectional technique. First, the iron nitride powder was mixed with G-1 epoxy (Gatan Inc.) on a Teflon sheet and the mixture was heated to 403 K on a hot plate. The mixture was spread using a Teflon stick to make a smooth thin film, which was heated for about 20 min. After cooling, the thin film was removed carefully. Rectangular silicon wafers with a cross section of 2×2 mm were then cut. The thin film was sandwiched between two silicon wafers and bonded as a stack with a thin layer of epoxy under the pressure of a special spring-loaded vice. Then, the sample stack was cut cross sectionally into slices with thickness of 200–300 μm and polished to a thickness of 80–100 μm. TEM discs of diameter 3 mm were trepanned from the slices, making sure that the sandwiched film was at the centre of the disc. The disc was ground to a thickness of 7–10 μm by dimpling, and bonded into a grid of a diameter of 3 mm if necessary. Finally, it was thinned by ion milling to produce the final TEM specimen with a hole in the sandwiched film. At the edge of this hole electron-transparent particles could be observed. Fig. 1 shows a bright-field image of a TEM powder sample prepared using the above method. Each particle is made up of several grains as indicated with different letters.

TEM observations were carried out in a JEM-ARM1000 transmission electron microscope operated at an accelerating voltage of 1 MeV with a base pressure of $3-5 \times 10^{-6}$ Pa. The degrading of image due to high-voltage observation was not severe in this iron nitride material especially under conventional TEM observation.

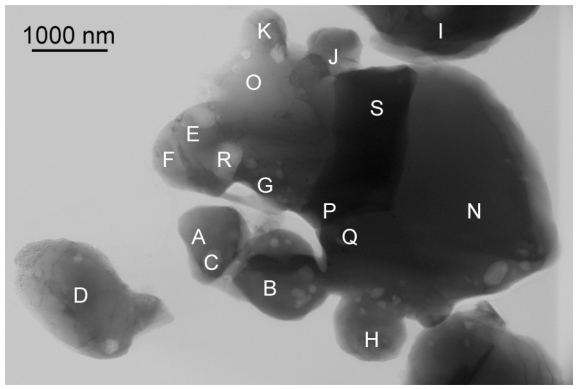

Figure 1 Bright-field image of iron nitride powders after annealing and quenching. The investigated grains are indicated by capital letters.

Both selected-area electron diffraction (SAED) and high-resolution electron microscopy (HREM) were used to identify the different phases.

3. Results

3.1. Superstructure of ε-$Fe_{2-3}N$ nitride

The iron atoms in ε-$Fe_{2-3}N$ exhibit a hexagonal close-packed arrangement (*hcp*) with nitrogen atoms occupying octahedral interstices. Different superstructures due to the ordering of nitrogen have been reported on the basis of X-ray powder diffraction patterns showing faint superstructure reflections: ε'-Fe_3N and ε'-Fe_2N with $a' = \sqrt{3}a$, $c' = c$, ε''-$Fe_{24}N_6$ and ε''-$Fe_{24}N_{10}$ with $a'' = 2\sqrt{3}a$, $c'' = c$ referred to the unit cell parameters a and c of the iron *hcp* structure [6–8]. In order to identify the superstructure in the ε phase, the TEM specimen was tilted using a double-tilt holder and electron diffraction investigations were carried out on different grains and particles in Fig. 1. Fig. 2 shows SAED patterns taken from grain J (a), grains I, P, and S (b), grain Q (c), and grain D (d). Using the basic *hcp* structure of iron in ε-$Fe_{2-3}N$, these patterns can be indexed as $[010]_{hcp}$, $[011]_{hcp}$, $[1\text{–}13]_{hcp}$, and $[1\text{–}14]_{hcp}$, respectively. Diffraction patterns of ε were also observed in grains F, K, and N. Therefore, in Fig. 1 grains D, F, I, J, K, N, P, Q, and S are ε-$Fe_{2-3}N$ grains.

In Fig. 2c and d, super-lattice spots appear at $1/3(110)_{hcp}$ and equivalent positions due to the ordering of nitrogen atoms in the *hcp* structure of iron. This indicates the formation of an ε' superstructure with unit parameters $a' = \sqrt{3}a$ and $c' = c$. Based on the ε' superstructure, the patterns in Fig. 2c and d can be indexed as $[031]\varepsilon'$ and $[014]\varepsilon'$, respectively. However, according to references [6, 9] two idealized basic superstructure types, labeled according to their ideally assigned compositions Fe_3N and Fe_2N, are possible for the ε' superstructure cell. The space group of the ideal ε'-Fe_3N superstructure is $P6_322$, while that of the ideal ε'-Fe_2N superstructure is

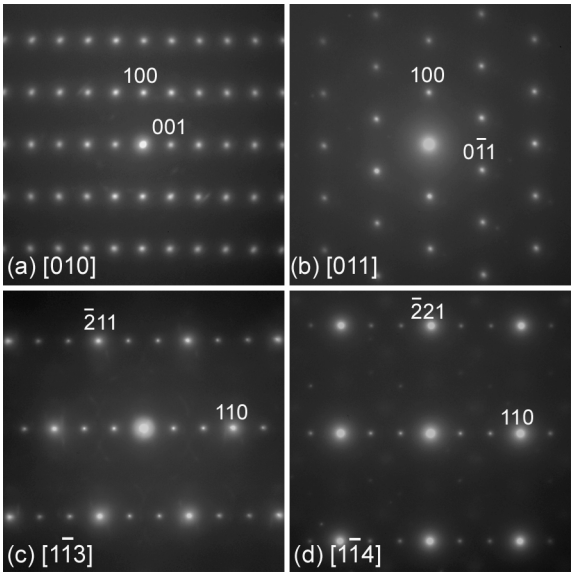

Figure 2 SAED patterns taken from ε-$Fe_{2-3}N$ grains, which were indexed with basic *hcp* crystal structure as (a) $[010]_{hcp}$, (b) $[011]_{hcp}$, (c) $[1\bar{1}3]_{hcp}$, and (d) $[1\bar{1}4]_{hcp}$. In (c) and (d) ε' super-lattice spots appear at $1/3(110)_{hcp}$ and its equivalent positions due to the ordering of nitrogen atoms.

$P\bar{3}1m$. The different distributions of nitrogen in the octahedral interstice in these two ideal superstructures lead to different diffraction patterns. For example, the (001)s (s—superlattice) class reflections (with $h, k = 3n$ and uneven l, hkl refer here to the superlattice) are absent for ε'-Fe_3N but appear for ε'-Fe_2N, while the (100)s class reflections (h-$k \neq 3n$ and even l) are present for ε'-Fe_3N but absent for ε'-Fe_2N. Fig. 3a shows a $[1\bar{1}0]_{hcp}$ SAED pattern, which can also be indexed as $[010]\varepsilon'$ based on the ε' superstructure. It can be seen that both (100)s (corresponds to the above-mentioned $1/3(110)_{hcp}$) and (001)s superlattice spots are present in the pattern. In order to determine whether these spots appear because of the superstructure or are due to double diffraction, the specimen was tilted around [001]s* by 5.38° in Fig. 3b and in a perpendicular direction around [100]s* by 6.94° in Fig. 3c. As indicated by arrow heads, the (001)s spot disappears in Fig. 3b but the (100)s spot remains present in Fig. 3c, which implies that the superstructure in this ε powder is ε'-Fe_3N type. This is in agreement with previous neutron diffraction investigations on powders having similar compositions as the ε-phase in this specimen of about $Fe_3N_{1.1}$ [13, 14]. This superstructure was also verified by the corresponding HREM image as shown in Fig. 3d. The contrast of (100)s planes appears at every three $(110)_{hcp}$ planes as indicated by arrow heads, but no contrast of (001)s plane can be seen at every two $(002)_{hcp}$ planes (also compare this HREM image with the corresponding SAED pattern in Fig. 3a). Others types of superstructures (e.g. ε'') were not observed in the ε grains of this specimen.

3.2. Precipitation of γ'-Fe_4N nitride

Electron diffraction was also conducted on other grains in Fig. 1, and it was confirmed that grains A, B, C, E, G, H, O, and R are γ'-Fe_4N nitride. These γ' grains precipitated from initial ε powders during the annealing process. Clearly the γ' and ε phases exist as individual grains within particles, which is different from the lamellar structure often observed in bulk samples [4, 15]. An enlarged image of grains A, B and C is shown in Fig. 4a. Grains A and B have a similar crystal orientation, while that of grain C is different. The SAED patterns of grains A and C are shown in Fig. 4b and d, and can be indexed $[100]\gamma'$ and $[122]\gamma'$, respectively. Fig. 4c is a diffraction pattern from an area including parts of both grain A and grain C using a larger selective aperture. White lines and

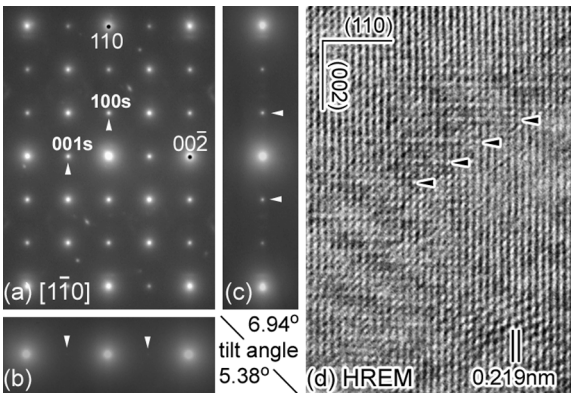

Figure 3 (a) SAED pattern of ε-$Fe_{2-3}N$ in $[1\bar{1}0]_{hcp}$ orientation. Considering the super-lattice spots, this pattern can also be indexed as [010]s. (b) Tilted pattern from (a) around [001]s* for 5.38°, showing the absence of (001)s and its equivalent spots. (c) Tilted pattern from (a) around [100]s* for 6.94°, showing the existence of (100)s and its equivalent spots. (d) HREM image corresponding to (a).

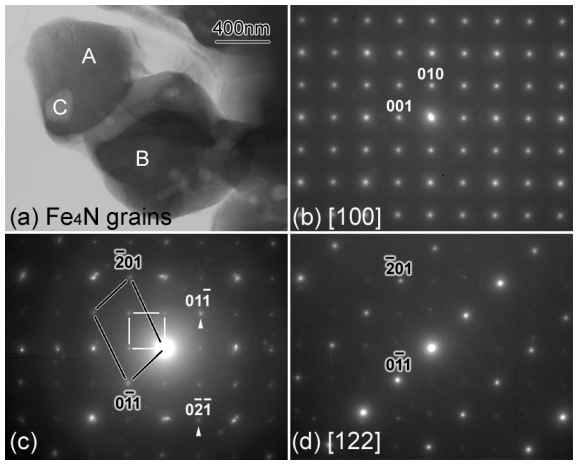

Figure 4 (a) Bright-field image of γ'-Fe_4N grains. (b) SAED pattern of grains A and B in $[100]\gamma'$ orientation. (c) SAED pattern including both grains A and C, showing the orientation relationship between them. (d) SAED pattern of grain C in $[122]\gamma'$ orientation.

letters are used to index the pattern of grain A, and black lines and letters are used to index that of grain C. The orientation relationship between the γ' grains A and C can be described as: $(0\bar{1}1)$a//$(0\bar{1}1)$c, (021)a//$(\bar{2}01)$c, and [100]a//[122]c.

Precipitation of γ' will lead to an increase in the lattice parameters of ε phase due to the increasing nitrogen content [16, 17]. According to TEM observations, γ' nitride forms only in a small number of the powder particles. Concentration variations are therefore expected among different particles with and without γ' precipitation. However, these variations are reduced by further annealing according to X-ray diffraction investigation [17]. Since transport of nitrogen through the gas phase is impossible because formation of N_2 is fully irreversible [18], the transfer of nitrogen atoms from powder particle to powder particle can only be realized via the direct mechanical contact of particles.

3.3. Orientation relationship between γ' and ε nitrides

Some particles contained both ε and γ' grains, and the orientation relationship between them was investigated. Fig. 5a shows an image of ε and γ' grains coexisting in a particle. An electron diffraction pattern taken from an area including both grains is shown in Fig. 5b. The spots of γ' are outlined with white lines and indexed with white letters, and those of ε are outlined with black lines and indexed with black letters. Again, the *hcp* crystal structure was used to index the ε phase and the ε' superstructure was not considered here. The orientation relationship between γ' and ε grains in this particle is $(11\bar{1})\gamma'//(\bar{2}0\bar{1})_{hcp}$, $[123]\gamma'//[010]_{hcp}$. A diffraction pattern taken from ε and γ' grains in another particle is presented in Fig. 6a, which shows an orientation relationship of $(11\bar{1})\gamma'//(11\bar{1})_{hcp}$, $[011]\gamma'//[112]_{hcp}$. The corresponding HREM image in this orientation is shown in Fig. 6b,

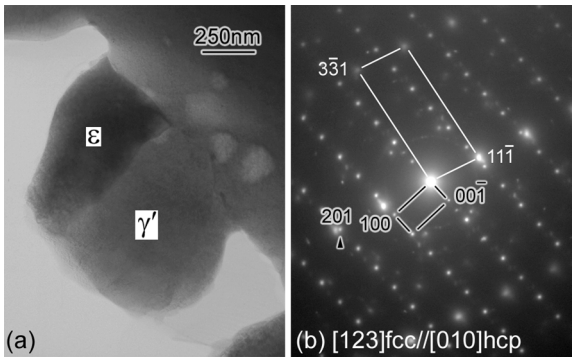

Figure 5 (a) Bright-field image of γ'-Fe_4N and ε-$Fe_{2-3}N$ grains. (b) SAED pattern including both ε and γ' grains showing the orientation relationship of $[123]\gamma'//[010]_{hcp}$. Spots of γ' are indicated with white lines and letters, and those of ε are indicated with black lines and letters.

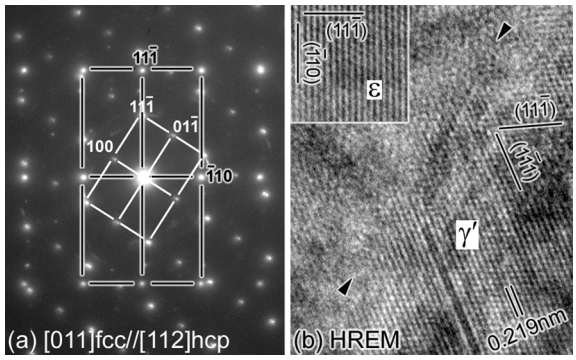

Figure 6 (a) SAED pattern showing the orientation relationship of $[011]\gamma'//[112]_{hcp}$. (b) The corresponding HREM image showing the interface between γ' and ε grains. Inset is the image of ε in a region away from the interface.

in which the interface (or grain boundary) between γ' and ε grains is indicated by arrowheads. The image of ε near the interface is not clear, which may be due to the overlapping of two grains since the grain boundary might not be edge-on. For comparison, the image of ε away from the interface is inserted in the top left corner of Fig. 6b. The $(11\bar{1})\gamma'$ planes, which according to the diffraction pattern are parallel to $(11\bar{1})_{hcp}$, have a spacing of only 0.132 nm and are not resolved in this image.

The orientation relationship between γ' and ε in the $\gamma'+\varepsilon$ lamellar structure in the compound layer of surface nitrided bulk sample has been reported to be $(1\bar{1}1)\gamma'//(001)_{hcp}$ and $[011]\gamma'//[010]_{hcp}$ [4]. If this relationship holds, the close-packed planes and close-packed directions in the *fcc* structure of γ'-Fe_4N are parallel to those in the *hcp* structure of ε-$Fe_{2-3}N$. Other parallel orientations between γ' and ε resulting from this orientation relationship can be determined from the stereogram shown in Fig. 7. Solid circles and small indices are for ε

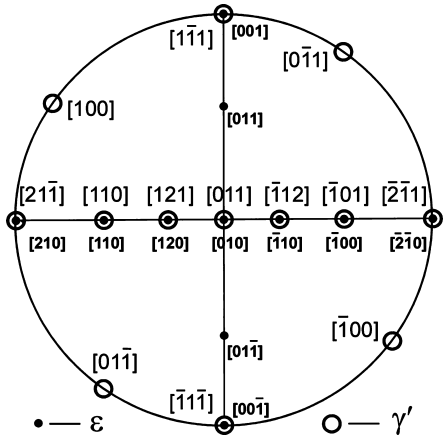

Figure 7 A stereogram showing the orientation relationship of $[011]\gamma'//[010]_{hcp}$ between γ' (open circles and large indices) and ε (solid circles and small indices) during phase transformation. This is the orientation relationship found in previous work on surface-nitrided bulk samples.

phase, and open circles and large indices are for γ' phase. It is clear that the observed orientation relationships found in our work and in Figs 5 and 6, are different from those in Fig. 7. In Fig. 5, ε-phase is in the $[010]_{hcp}$ orientation, but that of γ' is in $[123]\gamma'$ (not $[011]\gamma'$). When γ' was observed in $[011]\gamma'$ as shown in Fig. 6, the corresponding orientation of ε phase is $[112]_{hcp}$ not $[010]_{hcp}$. The transition matrix between γ' and ε for the orientation relationships shown in Figs 5 and 6 was also calculated. It was noted that they did not agree with each other, which implies that the orientation relationship in Fig. 5 is also different from that in Fig. 6. In fact, only a few γ' and ε grains were observed to have a simple orientation relationship, and they are not compatible with each other.

According to our TEM observations, there is no one simple, specific orientation relationship between γ' grains and the parent ε grains in the present specimens. This contrasts with the earlier reported orientation relationship of $(1\bar{1}1)\gamma'//(001)_{hcp}$ and $[011]\gamma'//[010]_{hcp}$ observed in $\gamma' + \varepsilon$ lamellae coexisting in one grain. In the surface-nitride bulk sample there is a nitrogen gradient from the surface to the interior, which should contribute to the precipitation of γ' in ε grains with a specific orientation relationship [4]. However, in the present case, γ' nucleates in or at a certain ε grain, and its growth involves long-range transport of nitrogen over distances of several grains or powder particles. This process is not homogeneous, which may result in variant orientation relationships as shown in Figs 5 and 6. A different mechanism should be considered for the precipitation of γ' in the presently investigated ε-powders.

4. Conclusions

1. TEM specimens of ε-$Fe_{2-3}N$ powders were successfully prepared by mixing the powders with epoxy and then sandwiching them between silicon wafers for ion milling.

2. According to electron diffraction and HREM investigations, the superstructure in ε phase is ε'-Fe_3N type, which is consistent with its initial composition of $Fe_3N_{1.0}$.

3. The precipitation of γ'-Fe_4N took place during the annealing of initially homogeneous ε powders, and γ'-Fe_4N was returned to room temperature by subsequent quenching. The newly formed γ'-Fe_4N phase coexists with ε the matrix as individual grains. Its morphology and orientation relationship with ε are different from those reported in bulk iron-nitride samples. In two individual cases, orientation relationships of $(11\bar{1})\gamma'//(\bar{2}0\bar{1})_{hcp}$ $[123]\gamma'//[010]_{hcp}$, and $(11\bar{1})\gamma'//(11\bar{1})_{hcp}$ $[011]\gamma'//[112]_{hcp}$ were observed between γ' and individual grains of ε. These orientation relationships are different from each other and from that reported between γ' and ε lamella, which is $(1\bar{1}1)\gamma'//(001)_{hcp}$ and $[011]\gamma'//[010]_{hcp}$. This suggests that a different nucleation and growth processes governs γ' precipitation in the presently investigated powder specimens.

Acknowledgment

A part of this work was supported by "Nanotechnology Support Project" of the Ministry of Education, Culture, Sports, Science and Technology (MEXT), Japan. The authors would like to thank Yoshiko Nakayama and Yumi Akiba for TEM sample preparation.

References

1. D. H. JACK and K. H. JACK, *Mater. Sci. Eng.* **11** (1973) 1.
2. E. J. MITTEMEIJER and M. A. J. SOMERS, *Surf. Eng.* **13** (1997) 483.
3. Z. Q. LIU, Y. X. CHEN, Z. K. HEI, D. X. LI and H. HASHIMOTO, *Metall. Mater. Trans.* **A 32** (2001) 2681.
4. Z. Q. LIU, Z. K. HEI and D. X. LI, *J. Mater. Res.* **17** (2002) 2621.
5. H. A. WRIEDT, N. A. GOKCEN and R. H. NAFZIGER, *Bull. All Phase Diagr.* **8** (1987) 355.
6. K. H. JACK, *Acta Crystallogr.* **5** (1952) 404.
7. S. B. HENDRICKS and P. B. KOSTING, *Z. Kristallogr.* **74** (1930) 511.
8. K. H. JACK, *Acta Crystallogr.* **3** (1950) 392.
9. Z. Q. LIU, D. X. LI, Z. K. HEI and H. HASHIMOTO, *Scripta Mater.* **45** (2001) 455.
10. *Idem.*, *ibid.* **46** (2002) 179.
11. J. D'HAEN, C. QUAEYHAEGENS, G. KNUYT, M. D'OLIESLAEGER and L. M. STALS, *Surf. Coat. Technol.* **74–75** (1995) 405.
12. D. GERARDIN, H. MICHEL, J. P. MORNIROLI and M. GANTOIS, *Mem. Sci. Rev. Metall.* **74** (1977) 457.
13. A. LEINEWEBER, H. JACOBS, F. HÜNING, H. LUEKEN, H. SCHILDER and W. KOCKELMANN, *J. Alloys Compound.* **288** (1999) 79.
14. A. LEINEWEBER, H. JACOBS, F. HÜNING, H. LUEKEN and W. KOCKELMANN, *ibid.* **316** (2001) 21.
15. D. GERADIN, J. P. MORNIROLI, H. MICHEL and M. GANTOIS, *J. Mater. Sci.* **16** (1981) 159.
16. T. LIAPINA, A. LEINEWEBER, E. J. MITTEMEIJER and W. KOCKELMANN, *Acta Mater.* **52** (2004) 173.
17. T. LIAPINA, A. LEINEWEBER, E. J. MITTEMEIJER, M. KNAPP, C. BAEHTZ, Z. Q. LIU, K. MITSUISHI and K. FURUYA, *Z. Krist. Suppl.* accepted.
18. E. LEHRER, *Z. Elektrochem.* **36** (1930) 383.